

# Chapter 20

## Climate Variability

J. Bendix(✉), R. Rollenbeck, P. Fabian, P. Emck, M. Richter, and E. Beck

### 20.1 Introduction

In this paper variability refers to the range of values between particular climate maxima and minima over a period of time (Mitchell 1976). Atmospheric variability in space and time can significantly alter the response of the ecosystem. For instance, comprehensive studies emphasise notable relations of reproduction phenology to climate in tropical rain forests (e.g. Hamann 2004). Three types of relevant spatio-temporal heterogeneities are discussed in this chapter:

1. Long-term and quasi-periodic oscillations of meteorological conditions;
2. Seasonal changes of selected meteorological parameters (clouds and precipitation), as a supplement to information already presented in Chapter 8;
3. The diurnal course of rainfall.

### 20.2 Results and Discussion

#### 20.2.1 *Quasi-Periodic Variability and Extreme Events*

Specific year-to-year variability, quasi-periodic oscillations and extremes of the meteorological parameters are of ecological importance for the study area. In this section we briefly discuss:

1. The influence of the quasi-periodic El Niño–Southern Oscillation (ENSO) phenomenon = El Niño (EN) and La Niña (LN) events;
2. Specific circulation patterns which lead to very low temperatures in the RBSF.

The analysis of rainfall and temperature data of several EN/LN events since 1972 in Ecuador has shown that the phenomenon mainly affects the coastal plains with floods (EN) or droughts (LN; e.g. Bendix 2000, 2004). Teleconnections to the highland and the eastern escarpment of the Andes are irregular and less clear. For the eastern slopes, a slight tendency exists towards reduced (EN) or enhanced (LN)

rainfall and positive (EN) or negative (LN) temperature anomalies. However, positive rainfall anomalies are still observed in the terminal EN phase (April to May). Unfortunately, no long-term time series of rainfall and temperature are available for the RBSF area. The latest strong EN/LN event (1998/1999) shows positive average temperature anomalies (+197% of  $1\sigma$  standard deviation) at the ECSF meteorological station in the terminal EN phase (April to May). In contrast to the observed deviation, enhanced average temperatures are registered also during LN 1999 (October 1998 to May 1999; +90% of  $1\sigma$  standard deviation). It is striking that the central LN phase (December 1998 to January 1999) shows significantly reduced minimum temperatures (-160% of  $1\sigma$  standard deviation). Rainfall at the ECSF/Cerro meteorological stations during the terminal EN and whole LN is nearly normal (EN -38%/-5%; LN +12/+8% of  $1\sigma$  standard deviation). Only January 1999 (central LN) reveals considerable positive rainfall anomalies. Monthly totals of rainfall during 1980–2000 are available for the station San Ramón (3°59'02" S, 79°05'12" W, 1820 m a.s.l.) in the Rio San Francisco valley close to ECSF. This period encompasses four EN (1972/1973; 1982/1983; 1986/1987, 1997/1998) and one LN (1998/1999). During all ENs, the San Ramon station reveals generally drier conditions than normal. LN 1998/1999 is characterised by slightly enhanced precipitation, especially in January, April and May 1999.

It is well known that extratropical cold air surges can affect the Tropics of South America (*friajes*; e.g. Breuer 1974) causing low temperatures in the RBSF area. The effects of such cold events, which last for 4–5 days on average, have been observed for the study area during the austral winter (May to October). During 1998 and 2001, 23 events could be registered. The coldest days and lowest temperatures ever observed in the ECSF area since the measurements began were related to cold air surges and featured the absolute minimum temperature of 0.7 °C at the climate divide (main ridge) in 3400 m a.s.l. and 3.9 °C at the Cordillera del Consuelo at 2930 m a.s.l. (11 July, 3 August 1999). The course of average hourly temperature and the synoptic situation during a strong cold air surge in August 1999 are presented in Fig. 20.1.

Cold events are introduced by the formation of a high pressure ridge from the South Pacific anticyclone over the Andes to the Pampa region (14 August) when cold air can intrude the Amazon area from the south (*friaje*). Such circulation patterns initiate the establishment of the south Atlantic anticyclone close to the east coast of southern South America (16–20 August), which is related to an equatorward cold air mass transport at the front of the high pressure system. The resulting cold SE trade winds affect the study area with a temporary complete cessation of rainfall and a significant drop in temperature, especially in the elevated parts.

### 20.2.2 Seasonal Variability

Cloudiness is a key factor in the climate system because of manifold feedbacks to the other meteorological parameters (Stephens 2005) and hence, of ecological

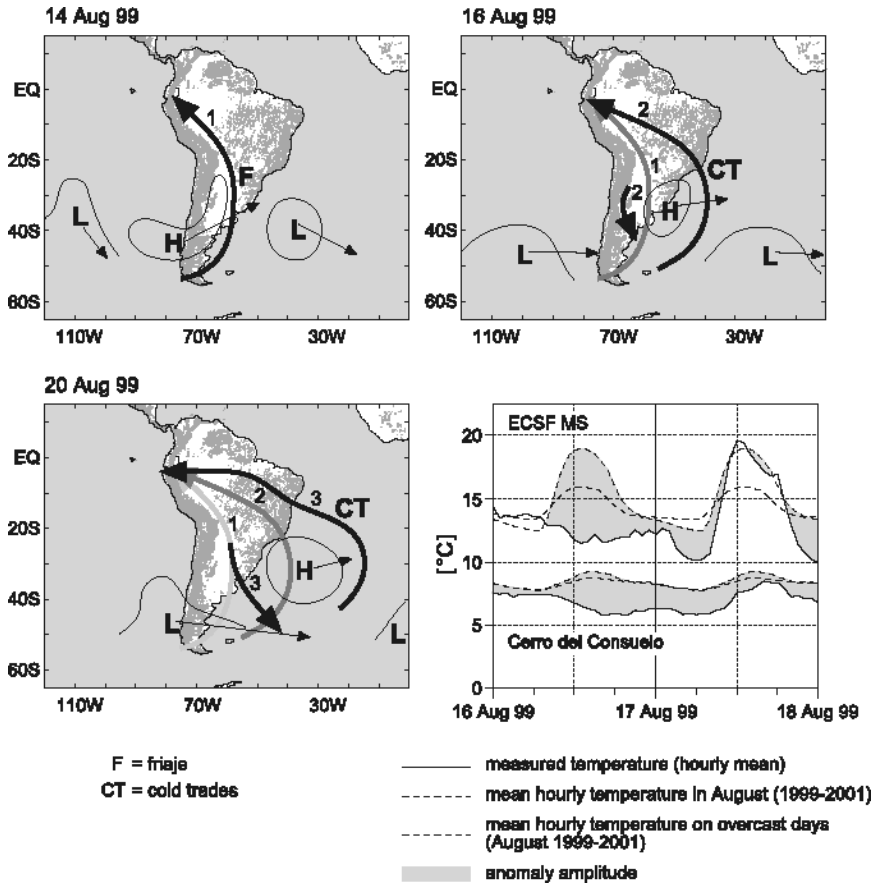


**Fig. 20.1** Synoptic weather situation (pressure distribution, streamflow at 850 hPa) during the cold event (14–20 August 1999) and air temperature development in the RBSF in comparison with average temperature

importance. Fog water deposition on the vegetation of tropical montane cloud forests is important for the hydrological cycle (Bruijnzeel 2001; Fleischbein et al. 2005). Modifications of the radiation balance (e.g. heat, UV-B and water stress by high transpiration rates in the absence of clouds) are of ecological importance (e.g. Alados et al. 2000). Some authors demonstrated that enhanced UV-B intensities during clear-sky conditions in some cases decrease, advance or delay (depending on species) the time of flowering (e.g. Caldwell et al. 1998). Flowering and fruit production are synchronised with drought periods and sunny conditions because the absorption of photosynthetically active radiation (PAR) by clouds in the wet season limits the reproduction potential, due to the low accumulation of resources through photosynthesis (e.g. Wright et al 1999; Hamann 2004).

The study area is characterised by a strong gradient of cloudiness in space and time (Bendix et al. 2004b, 2006a). The main chain of the Cordillera Real clearly separates the basin of Loja with reduced frequencies from the area of the Rio San Francisco where the average cloud frequency can exceed 85%. Cloudiness increases along the altitudinal gradient from the valley bottom of the Rio San Francisco to the Cerro del Consuelo. It is especially high when the slopes are exposed to the predominating easterly streamflow due to blocking effects. In contrast, the leeward escarpment is mostly characterised by a reduced cloud amount. The seasonal cloud distribution completely changes from Loja to the Cerro del Consuelo (distance in a straight line <20 km). The area west of the main Cordillera is characterised by a maximum of cloud frequency in austral summer (December–February, DJF) and a secondary peak in the austral spring (September–November, SON). The transition zone between both cloud regimes is marked by the stations of El Tiro and Cajanuma where a third peak in cloud frequency begins to emerge in the austral winter (June–August, JJA). This peak becomes specifically dominant in the Amazon-exposed part of the study area (Cerro del Consuelo). Cloud frequency is high throughout the year at the altitudinal level around 3000 m a.s.l.

The same tendency of seasonal variability in space and time can be observed for rainfall (Fig. 20.2). Generally, the main cordillera separates the moist Amazon-exposed easterly slopes from the drier inner-Andean areas of Loja and Catamayo. However, clear differences can be observed between the austral winter (JJA) and summer (DJF). The highest rainfall amounts in the austral winter (JJA) occur at

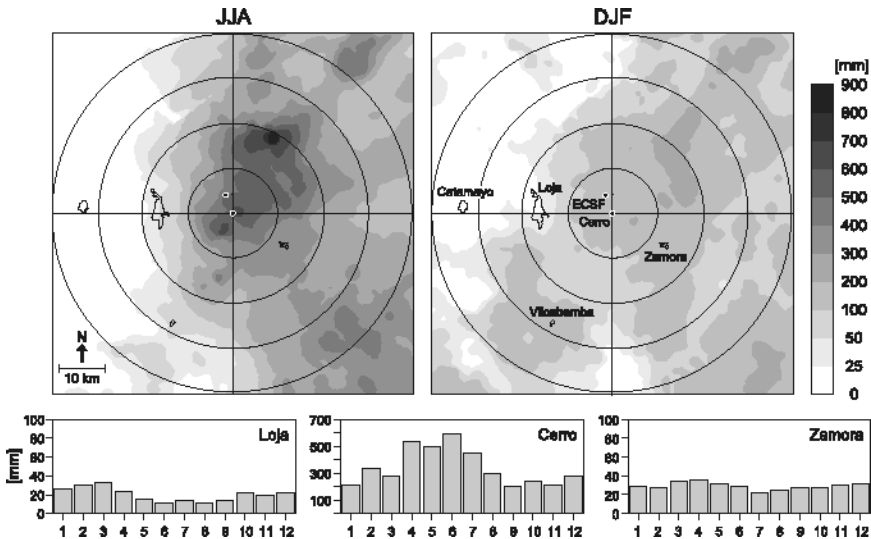


**Fig. 20.2** Average distribution of rainfall for the austral winter (JJA June+July+August) and summer (DJF December+January+February) derived from X-band Radar (top, period March 2002 to July 2003); and registered rainfall at Loja (2160 m a.s.l.), Cerro del Consuelo (2930 m a.s.l.) and Zamora (970 m a.s.l.) meteorological stations (bottom)

steep slopes well exposed to the prevailing easterlies northeast of the study area. This applies also to the extremely exposed Cerro del Consuelo, the highest peak of the central study area, which shows lower average cloud top heights and standard deviations during this season (see Bendix et al. 2006b). The rainfields in the LAWR maps show a homogenous structure but rainfall slightly decreases towards the Amazon lowlands. It should be stressed that extreme amounts of rainfall recorded by rain gauges in the highest part of the Cordillera about 15 km south of the study area are not reproduced by the radar maps because of the beam obstruction of this sector (Rollenbeck and Bendix 2006). Cloud and rain formation in the austral winter (JJA) is of predominantly orographic character and is linked to the high wind speed in the upper parts of the study area (see Chapter 8 in this volume) which imply high condensation rates.

The analysis of wind direction and rain intensity/rain frequency confirms the complex structure of seasonal variability in precipitation dynamics. Figure 20.3 illustrates that easterly streamflow predominates in the study area throughout the year. While in the austral winter almost no westerly streamflow occurs, the portion of weather situations with winds from the western sector increases up to ~40% in October–November. It is striking that the easterly streamflow from May to September is related to a general high frequency of rainfall per hour. The average rain intensity decreases especially during the austral winter (JJA). In contrast, a lower precipitation frequency is also observed at the end of the year when westerly circulation patterns become significant. The low frequency is related to higher rain rates (especially in November) which points to a more convective situation.

A tracking analysis of rain cells using a series of consecutive radar images illustrates the variation in the rainfall dynamics of different seasons. The rain cells in August (Fig. 20.4, right) mainly originating from lower cap clouds move in an east–west direction but are blocked at the main crest of the Cordillera. On the leeward side, reminders are rapidly dissipated due to the lee effect. Hence, cell trajectories terminate in this area. During such situations, the windward slopes are exposed to high amounts of orographically enhanced rainfall, especially in the upper parts of the study area.

The example of westerly cell propagation (Fig. 20.4, left) is related to convective cells over the whole area west and east of the crestline of the Cordillera Real. However, the reduction in propagation speed and the change in direction points out that the elevated topography also plays an important role for the rainfall dynamics from higher clouds during westerly circulation patterns.

Clear sky conditions are the most effective between October and January by air flows from the northwest, which are termed “Veranillos del Niño” (Fig. 20.3, lower panel). An associated strong subsidence over the cordillera causes extraordinary aridity particularly in the highlands. The large saturation deficit results in an extreme water stress for the vegetation (during 1998–2001 the regional absolute minimum of 11.8% relative humidity recorded at 3400m a.s.l. is linked with a Veranillos del Niño event). As Veranillos del Niño can last up to three weeks and return relatively regularly, it is quite probable that apart from strategies against the common extreme humid conditions and high wind speeds, vegetation has also been

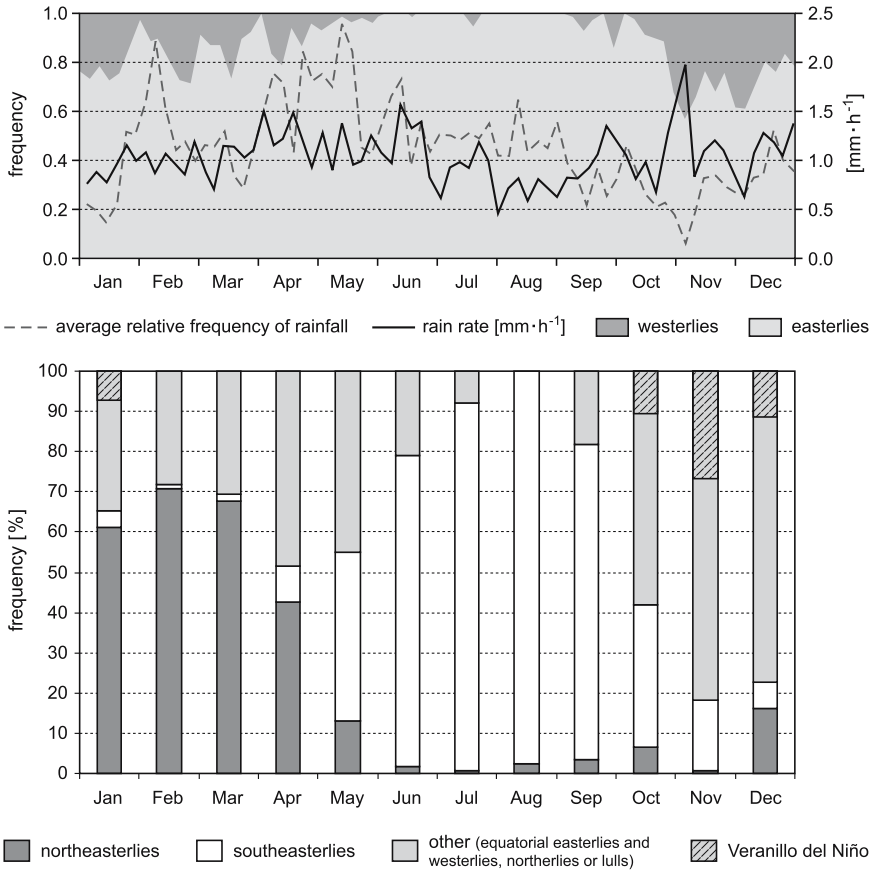


**Fig. 20.3** Frequency of wind direction, average relative frequency of rainfall and average rain rate at the Páramo meteorological station (January 1998 to February 2005, *top*). *Bottom* Mean monthly frequency of synoptic winds at 850hPa over west equatorial South America during 1998–2001, interpreted from daily average wind patterns between 65°S–30°N and 150°W–15°E from NCEP Re-analysis data

forced to adapt strategies against peak water stress situations. After several days of Veranillo del Niño conditions, even the mountain rain forests in the east become desiccated to such a degree that they can catch fire – a circumstance all too often exploited by the local population.

### 20.2.3 Diurnal Variability

Variability in weather patterns is not only present throughout the year but also throughout the diurnal cycle. This can be exemplarily illustrated by radar images of the spatio-temporal rainfall distribution (Fig. 20.5).

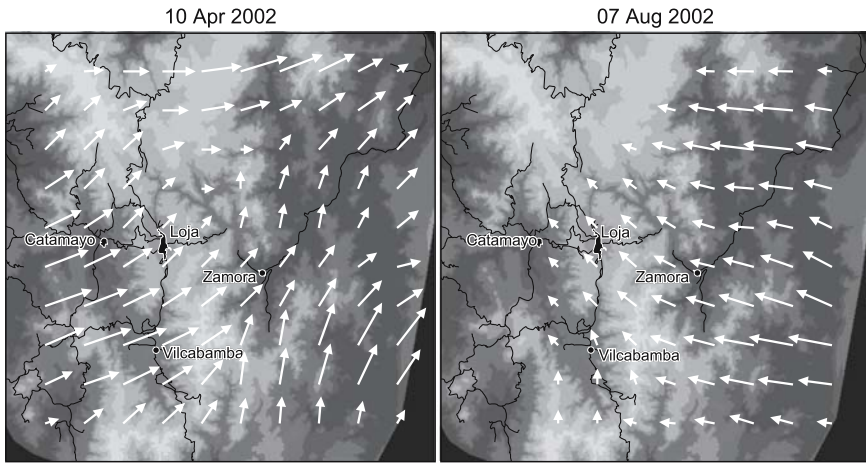


**Fig. 20.4** Representative trajectories of rain cells for a weather situation with easterly impact in JJA (*right*, 7 August 2002) and westerly impact in FMA (*left*, 10 April 2002) derived from LAWR storm cell tracking. The length of the arrows is proportional to the displacement of the centre of individual cells. These displacement patterns are the result of the absolute wind driven movement of the cells, including the internal motion of the cloud systems. It should be stressed that the arrows do not represent the wind field itself

In the austral winter (JJA), rainfall affects the entire study area at the windward eastern escarpment, with a maximum in the early morning hours (0600 hours, local time) and in the upper parts of the study area close to the ECSF station. The diurnal cycle in the austral summer (DJF) shows an inverse behaviour. Rainfall is stronger in the late afternoon (1800 hours, local time), spatial patterns differ as well. While early morning precipitation is centred in the upper part of the central study area and is mainly restricted to the area east of the main Cordillera, the afternoon peak shows a clear cellular-convective structure which is partly related to thermal valley-breeze systems. However, the centres of main rainfall activity are the lower parts of the study area east of the Cordillera as well as the basins of Loja and Vilcabamba west of the main Cordillera crest.

Examination of the diurnal cycle in the free atmosphere over the ECSF research station by using a vertically pointing rain radar profiler (MRR) reveals a unique situation of the study area (see Bendix et al. 2006a). Average rainfall is generally low throughout the day. However, two clear maxima can be recognised with a main peak around sunrise (0530–0630 hours, local standard time; LST) and a secondary peak in the early afternoon hours at 1430–1530 hours LST. A third period of above average precipitation is observed at 2300–2330 hours LST. The relatively low rainfall frequency and the high maximum at e.g. 1730–1800 hours or 2030–2100 hours LST points to the occasional occurrence of stronger convective events, triggered by the up-slope breeze system. The precipitation peak around sunrise reveals the greatest variability in rainfall and rain frequency, being characterised by different stratiform and convective mechanisms of rainfall formation.

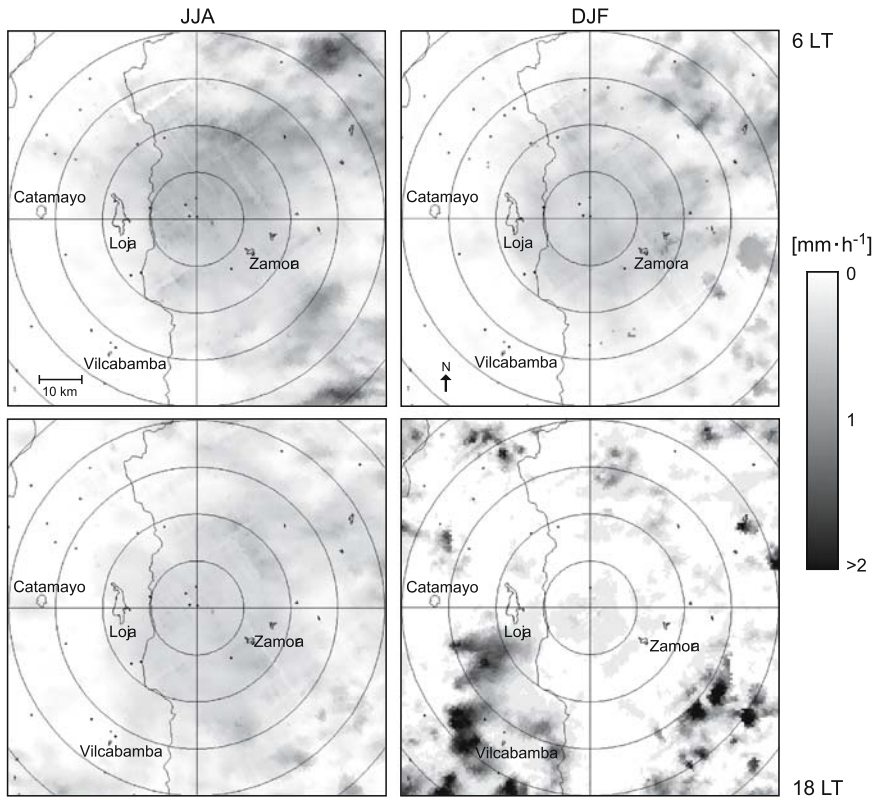


**Fig. 20.5** Distribution maps of rainfall for selected periods in austral winter (*JJA* June+July+August 2002) and summer (*DJF* December+January+February 2002/2003) at 0600 hours and 1800 hours, local time (LT), derived from X-band Radar. The images are based on the average rainrate from 0500 hours to 0655 hours LT and from 1700 hours to 1855 hours LT for all days of the given periods

Inspecting the average vertical profiles of rainfall for the two peak times (Bendix et al. 2006a, Fig. 6), the maximum in the vertical profile is observed for the fifth level at 1347 m above the ECSF station (= 3207 m a.s.l.). The comparison of the situation at 0600 hours and 1500 hours LST reveals interesting differences in the vertical stratification. The shape of the vertical profile during the afternoon maximum is quite similar to the daily mean, but shows a slightly higher decrease in rainfall of 39% from the maximum zone at ~3200 m a.s.l. down towards to the ECSF station. This decrease is clearly less pronounced (16%) during the pre-dawn/dawn maximum where a significant reduction of rainfall amount is observed only in the lowest two levels. The shape of the profiles and further investigations of droplet spectra and satellite images (Bendix et al. 2006b) points to different rain generating processes. The afternoon peak is clearly related to convective processes. Rainfall is formed in the upper atmospheric levels (>3200 m a.s.l.) and droplets



mainly originating from the stratiform area of the cells partly evaporate on their way to the valley bottom. The weak gradient for the morning peak at the valley bottom (which turns to an afternoon maximum at the crest levels) is most likely a product of complex mesoscale dynamics (Bendix et al. 2006b). As a result, rain clouds can overflow the bordering ridges of the Cordillera del Consuelo providing rains of higher intensity at the ECSF research station. We hypothesise that the seeding of fog and low stratus clouds, which form due to nocturnal radiation processes in the valley, by the upper-level rain clouds, can lead to continuous droplet growth right down to the near surface layer.

#### ***20.2.4 Weather Variability and Tree Phenological Response***

A high degree of intra- and interspecific synchronisation of phenological traits was noticed for flowering and fruiting of 12 tree species in the study area. Just a short summary of results can be given in this paper. The whole study is presented by Bendix et al. (2006c).

Apart from one species that flowered more or less continuously, two groups of trees could be observed, of which one flowered during the less humid months (SO) while the second group started to initiate flowers towards the end of that phase and flowered during the wettest season (AMJJ). Phenological events of most of the plant species showed a similar periodicity of 8–12 months which followed the annual oscillation of relatively less and more humid periods and thus were in phase or in counter-phase with the oscillations of the meteorological conditions. Periods of unusual cold or dryness, presumably resulting from underlying longer-term trends or oscillations affected the homogeneity of quasi-12-month flowering events, fruit maturation and also the production of germinable seeds. Some species indicate underlying quasi-two-year oscillations which are synchronised with the development of e.g. air temperature, others reveal an underlying decrease or increase of flowering activity over the observation period, influenced e.g. by solar irradiance.

### **20.3 Conclusions**

With regard to meteorological variations in space and time, it is shown that the ENSO phenomenon does not cause extraordinary weather anomalies in the RBSF area. In general, LN situations seem to induce somewhat stronger effects. Extratropical cold air surges can affect the study area, mainly in the austral winter with a significant reduction of air temperature, especially in the crest areas. Both findings underline the strong influence of the Atlantic circulation on the study area and the effect of the Andes which shelter the eastern Andean slopes from Pacific airmasses most of the time.

Rainfall and cloudiness reveal marked season-specific spatial patterns. Unexpectedly, the analysis of cloudiness, rainfall dynamics and wind field reveal that the JJA maximum in precipitation is mainly a result of an orographic lifting of moist air masses on the eastern Andean slopes. It is striking that the diurnal course of rainfall shows a unique behaviour for the RBSF area. A pre-dawn/dawn maximum and a secondary afternoon peak is observed for rainfall at the ECSF station. The morning maximum is probably a result of mesoscale dynamics in combination with local effects. However, the exact mechanisms must be investigated in future studies.

The phenological cycle for the most investigated trees is clearly associated with the seasonal course of the weather (temperature, radiation, precipitation). However, most species are affected by longer-term cycles which are probably related to climatic oscillations.